Projection of semi-shapes for rotational symmetry detection

Thanh Phuong Nguyen[1], Thanh Tuan Nguyen[1,2], Thanh-Hai Tran[3]

[1] Université de Toulon, Aix Marseille Univ, CNRS, LIS, Marseille, France
[2] HCMC University of Technology and Education, Faculty of IT, Thu Duc City, HCM City, Vietnam
[3] School of Electrical and Electronic Engineering, Hanoi University of Science and Technology, Hanoi, Vietnam
Email: tpnguyen@univ-tln.fr; tuannt@hcmute.edu.vn; hai.tranthithanh1@hust.edu.vn

***Abstract*—A novel method for detecting rotational symmetry is addressed in this paper by introducing a new concept of semi-shapes to overcome the main problem of projection-based approaches for studying rotational symmetric properties of an arbitrary shape. It is due to the fact that in the classical approaches, projection cues are periodical with a period of π preventing exploitation of rotational properties. We then propose the profile of semi-shapes as a signature of the shape together with a simple yet efficient technique to determine the rotation symmetry of an arbitrary shape by considering the correlation of this signature and its circular shift. A new measure is also introduced to determine how good the rotational symmetry would be. Experiments on single/compound-contour shapes have clearly corroborated the efficacy of our proposal.**

***Index Terms*—rotational symmetry detection, $\mathcal{R}$-signature, Radon transform**

I. Introduction

Symmetric structures are omnipresent (e.g., in man-made products, biological objects, etc.) and usually attract human attention. As one of the basic features of shapes and objects, symmetry plays an important role in shape analysis and other fields of computer vision. Symmetrical shape descriptions and the symmetrical feature detection of objects are very useful in shape matching, model-based object, and recognition applications. Many approaches [1]–[17] have been introduced for analyzing symmetric features. Based on the shape information, we can generally categorize these approaches into two main types of symmetry detection as follows.

The first category consists of methods that detect the reflectionally and/or skewed symmetric characteristics of shapes. Ogawa [1] proposed to detect the symmetric axis of shapes by using symmetry analysis of line drawings based on Hough transform. Yip [2] then improved this approach to deal with both reflectional and skew symmetry. Also based on the Hough transform, Lei and Wong [3] tried to detect and recover the pose of reflectional and rotational symmetry from a weak single perspective image. In other aspects, Cornelius and Loy [8] detected bilateral symmetry in images under perspective projection by matching pairs of symmetric features. Nagar and Raman [15] proposed an energy minimization approach to detect multiple reflectional symmetries, while in another work [16], they addressed optimization on the manifold for a set of points to determine approximately reflectional symmetry. Based on analyses of shape signatures, Nguyen *et al.* [17] recently presented robust detectors that can point out the multiple reflectional symmetries of binary shapes constructed by complex contour-based components.

For the second category of the symmetry detection, several techniques have been proposed to deal with detecting the rotational properties of shapes. Leou and Tsai [18] considered a number of intersection points, resulted by the different kinds of the centroid circles of a given closed-curve shape, to determine the actual order of rotational symmetry. Also based on the point analyses, Lin *et al.* [19] proposed fold-invariant shape-specific points for detecting the orientations of rotationally symmetric shapes, while Loy and Eklundh [6] grouped symmetric pairs of feature points and characterized the symmetries presented in an image. In terms of addressing transformations in the shape analysis, Flusser and Suk [20] introduced a new set of moment invariants which are invariant against the similarity transforms for recognition of objects having n-fold rotation symmetry, whilst Yip [21], [22] utilized the transforms of Hough and Fourier to extract local features of an arbitrary shape so that the detectors can be against noise and occlusion. In other aspects, Cornelius and Loy [7] detected planar rotational symmetry under affine projection. Prasad and Davis [5] localized multiple rotational symmetry axes in natural images using gradient magnitudes.

Recently, Aguilar *et al.* [23] took advantage of the Slope-Chain-Code (SCC) theory [24], [25] to represent the curve of binary shapes for an issue of rotational symmetry detection. The SCC-based detector was then verified on a small set of rotationally symmetric shapes of MPEG-7 [26]. In fact, this detector just works on binary shapes with a single contour. It would not be on the compound shapes with complex contour-based parts due to its inherent restriction in the analysis of shape's contours. In addition, the traditional methods [17], [27], based on $\mathcal{R}$-signature [28] to analyze a given shape, are not adaptive to a rotational symmetry application. This is because the periodical attribute with a period of π is an internal limitation of the $\mathcal{R}$-signature in consideration of the entire shape's area.

To deal with the aforementioned drawbacks, we introduce in

Accepted by ICPR'2022

this work an efficient method for rotational symmetry detection by addressing the following novel concepts. *i)* The correlation of the profile of semi-shapes, obtained by a decomposing operation of a given binary shape, is proposed to detect symmetric properties. The $\mathcal{R}$-signature of these semi-shapes permits us to overcome the conventional issue of the projection-based methods, whose projected features would be the same after a rotation of angle π. *ii)* A rotational symmetry measure ranging from 0 to 1 is proposed to estimate how good the symmetry is. Experiments have validated that our proposed detector can work well in detecting the rotational symmetry on binary shapes, particularly those with complex contour components compared to the recent contour-based method.

II. Radon transform

Let f, defined on $\mathbb{R}^2$, be a 2D function and $L(\theta,\rho) = \{\mathbf{x} \in \mathbb{R}^2 \mid \mathbf{x}\cdot\mathbf{n}(\theta) = \rho\}$ be a straight line in $\mathbb{R}^2$, where θ is the angle that L makes with the y axis, $\mathbf{n}(\theta) = (\cos\theta, \sin\theta)$, and ρ is the radial distance from the origin to L. The Radon transform [29] of f, denoted as $\mathcal{R}_f$, is a function defined on the space of lines $L(\theta,\rho)$ by calculating the line integral as follows.

$$\mathcal{R}_f(\theta,\rho) = \int f(\mathbf{x})\,\delta(\rho - \mathbf{x}\cdot\mathbf{n}(\theta))\,\mathrm{d}\mathbf{x} \tag{1}$$

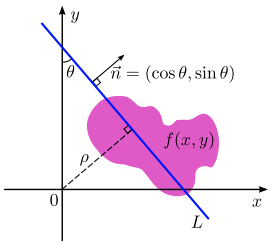

Fig. 1. Radon transform.

In the shape analysis, the function f is constrained to take value 1 if $\mathbf{x} \in \mathcal{D}$ and 0 otherwise, where $\mathcal{D}$ is the domain of the binary shape represented by f (see Fig. 1).

$$f(\mathbf{x}) = \begin{cases} 1 \text{ if } (\mathbf{x}) \in \mathcal{D} \\ 0 \text{ otherwise} \end{cases} \tag{2}$$

Radon transform is robust to additive noise and some other good geometric properties [29], which have been exploited in different works [27], [30]–[33] of shape analysis. Tabbone *et al.* [28] introduced a shape signature, called $\mathcal{R}$-signature, for an effective shape representation as follows.

$$R_{f2}(\mathcal{D},\theta) = \int_{-\infty}^{+\infty} \mathcal{R}_f^2(\theta,\rho)d\rho \tag{3}$$

Fig. 2 illustrates the $\mathcal{R}$-signatures of two binary shapes. Please refer to [28] for more illustrations about the robustness of $\mathcal{R}$-signature against additional noise and non-linear deformations. Hereunder, we recall two properties of $\mathcal{R}$-signature as follows.

- *Periodicity:* R_{f2} is periodical with the period of π.
- *Rotation:* A rotation of the image by an angle θ_0 leads to a circular shift of R_{f2} of θ_0.

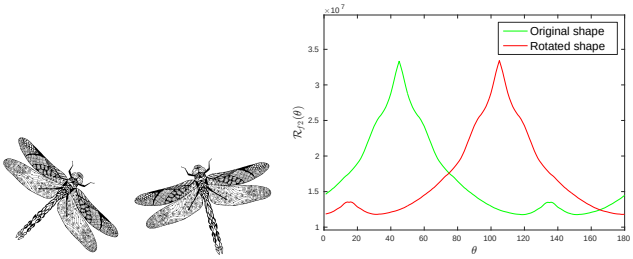

(a) Input (b) Rotated (c) $\mathcal{R}$-signatures

Fig. 2. Illustration of $\mathcal{R}$-signatures [28].

III. Rotational symmetry detection

A. Limitations of projection-based approaches

We point out the limitations of projection-based approaches in the detection of rotation symmetry. The following analyses address $\mathcal{R}$-signature as an example, but they are also valid for other projection-based methods which share the same limitations because the projected features are the same after a rotation of angle π. This prevents the detection of 2-order rotation shapes with their angles of rotation π. Concretely, a projection-based shape signature, such as $\mathcal{R}$-signature, has the following issues to detect rotational symmetric properties.

1) First, due to [28], $\mathcal{R}$-signature ($R_{f2}(\mathcal{D},\theta)$) is periodic with respect to θ with period π thanks to semi-periodic property of Radon transform. Therefore, a shape having a rotation symmetry of angle π is not detected by addressing cyclic symmetry in its $\mathcal{R}$-signature.
2) Second, the cyclic period of $\mathcal{R}$-signature does not always correspond to the angle of rotation symmetry. For example, if a shape has a rotation symmetry of angle $\frac{2\pi}{3}$, it must be the same after a rotation of $2 \times \frac{2\pi}{3} = \frac{4\pi}{3}$. In addition, its $\mathcal{R}$-signature is also cyclic periodic with period π. It can be deduced that the $\mathcal{R}$-signature of this shape has a cyclic symmetry of period $\frac{\pi}{3}$. Thus, detecting the cyclic period of $\mathcal{R}$-signature does not allow determining the angle of rotation symmetry of a shape. Figs. 3.(a)-(b) illustrate this example where the cyclic period of its $\mathcal{R}$-signature is not $\frac{2\pi}{3}$. In the meanwhile, Figs. 3.(c)-(d) show a 4-order rotation shape with a cyclic period of $\frac{2\pi}{4} = \frac{\pi}{2}$ as expected.

B. Novel framework based on projection of semi-shapes

The above limitations naturally come from the properties of the projection-based approaches. Indeed, a projection is only defined by its direction whilst its orientation is ignored. Those would be the obstacles of using $\mathcal{R}$-signature for a direct application of rotation symmetry detection. To deal with these problems, we propose hereunder a novel concept of semi-shape projection to adapt $\mathcal{R}$-signature for rotational symmetric properties of an arbitrary shape.

Definition 1. *A semi-shape of $\mathcal{D}$ in direction $\theta \in [0, 2\pi)$, called $\propto^\theta(\mathcal{D})$, is defined as a part of $\mathcal{D}$ which is on the left side of the line in direction θ passing through $\mathcal{D}$'s centroid.*

Accepted by ICPR'2022

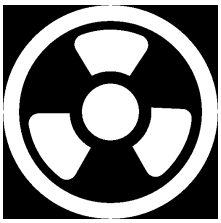

(a) A 3-order rotation shape

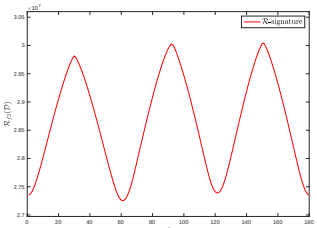

(b) Its $\mathcal{R}$-signature has a cyclic period of $\frac{\pi}{3}$

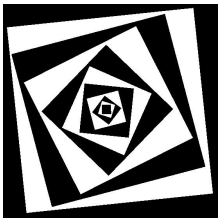

(c) A 4-order rotation shape

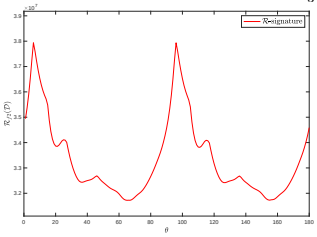

(d) Its $\mathcal{R}$-signature has a cyclic period of $\frac{2\pi}{4} = \frac{\pi}{2}$

Fig. 3. The cyclic period of $\mathcal{R}$-signature of a 3-order rotation shape is not $\frac{2\pi}{3}$ while that of 4-order rotation shape is $\frac{\pi}{2}$.

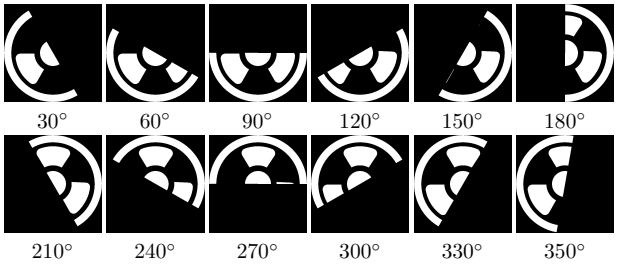

Fig. 4. Semi-shapes constructed from the shape in Fig. 3(a).

Fig. 4 presents a series of semi-shapes of a shape. From this figure, we could make the following findings.

- $\mathcal{D}$ is rotationally symmetric with angle θ_0 if and only if $\propto^{\theta}(\mathcal{D})$ and $\propto^{\theta+\theta_0}(\mathcal{D})$ are identical, $\forall\theta \in [0, 2\pi)$
- Generally, $\propto^{\theta}(\mathcal{D})$ and $\propto^{\theta+\pi}(\mathcal{D})$ are not the same.

The above findings allow us to address hereunder a new approach for rotation symmetry detection. For the simplicity, the interval $[0, 2\pi)$ is quantified into 360 directions: $\Theta = \{0°, 1°, 2°, \ldots, 359°\}$. Let us consider a signature of $\mathcal{D}$, called the profile of semi-shapes, as follows:

$$\zeta(\mathcal{D}, \Theta) = \{R_{f2}(\propto^{\theta}(\mathcal{D}), \theta)\}_{\theta\in\Theta} \quad (4)$$

Contrariwise to $\mathcal{R}$-signature [28], the profile of semi-shapes $\zeta(\mathcal{D}, \Theta)$ is not automatically cyclic symmetric with period $180° = \pi$. In addition, if it contains cyclic symmetry with period of θ_0, $\mathcal{D}$ is also rotational symmetric with angle θ_0.

Fig. 5 presents a study of rotation symmetry of shape in Fig. 3(a), which is based on the profile of its semi-shapes addressing 360 directions from 0° to 359° (see Fig. 5(a)). It could be seen from this figure that the profile is cyclic symmetric with a period of $120° = \frac{2\pi}{3}$, instead of $\frac{\pi}{3}$, as seen by its $\mathcal{R}$-signature (refer to Fig. 3(b)).

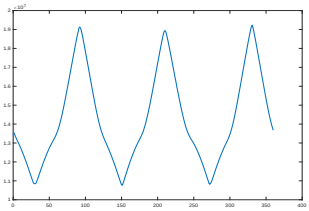

(a) Profile of semi-shapes

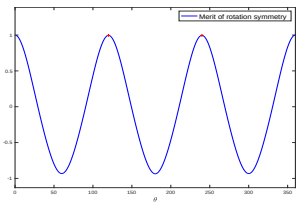

(b) Merit of rotation symmetry

Fig. 5. Detection of rotation symmetry.

C. Proposed method for rotation symmetry detection

Based on the analysis in the aforementioned sections, we propose a new method for rotational symmetry detection of an arbitrary shape $\mathcal{D}$ by considering the profile of its semi-shapes $\zeta(\mathcal{D}, \theta_0)$. The main idea is to measure the similarity between it and its circular shift of each angle θ, i.e., $\zeta(\mathcal{D}, \theta+\theta_0)$. If this similarity is perfect, we could confirm that the studied shape has not been changed after a rotation function at its center with the angle θ_0. In order to measure the similarity between $\zeta(\mathcal{D}, \theta_0)$ and $\zeta(\mathcal{D}, \theta+\theta_0)$, we propose to use Pearson's Linear Correlation Coefficient (PCC) [34]. These correlation values can range from –1 to +1, where a close-to-(+1) coefficient indicates a perfect positive correlation.

To exploit the proposed idea, we introduce Algorithm 1 for rotational symmetry detection of an arbitrary shape $\mathcal{D}$. Accordingly, the profile of semi-shapes $\zeta(\mathcal{D}, \Theta)$ is constructed to discover its rotational symmetric properties. The merit profile is calculated from the correlation between $\zeta(\mathcal{D}, \theta_0)$ and each its circular shift of angle θ using Pearson's correlation. The peaks of this merit profile are detected and refined by a threshold $\tau \in (0, 1)$. The number of peaks determines the order of rotation symmetry while the intervals between these peaks define the rotation order, and the mean of the detected peaks is reported as the measure of rotational symmetry. A MATLAB code demo for our proposed algorithm can be found at http://tpnguyen.univ-tln.fr/download/ICPR2022Rota.

IV. Experiments

A. Synthetic shapes

We first conduct experiments of synthetic shapes to verify the proposed rotational symmetry measure. Three synthetic subsets are considered for this purpose (see Fig. 6). Therein, subset S_1 consists of rotational symmetric shapes generated from regular polygons. S_2 includes the deformed shapes created from S_1 by addressing heavily additional noise (SNR = 1). S_3 contains shapes of non-regular polygons.

Fig. 7 shows some representative experiments on synthetic shapes. The line (a) (resp. (b), (c)) presents a shape of S_1 (resp. S_2, S_3) along with the profile of its semi-shapes and merits of rotation symmetry. This allows making several findings as follows. Thanks to the robustness of the profile of its semi-shapes against non-linear deformations, the corresponding merit of rotation symmetry is also robust against them (see lines (a) and (b) of Fig. 7). For the non-rotational symmetric shape (see line (c)), its profile does not contain any cyclic

Accepted by ICPR'2022

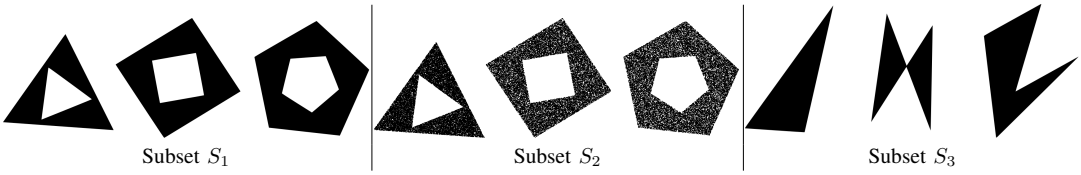

Fig. 6. Subsets of synthetic shapes.

Algorithm 1 Rotational symmetry detection of a shape $\mathcal{D}$.

Input: $\mathcal{D}$ – an arbitrary shape, τ – a refining threshold.
Output: ψ – rotational symmetric measure, θ_0 – the angle of rotation

1: Determine the centroid $C_{\mathcal{D}}$ of shape $\mathcal{D}$
$sX = \sum_{p\in\mathcal{D}} p_x$; $sY = \sum_{p\in\mathcal{D}} p_y$; $s = \sum_{p\in\mathcal{D}} 1$; $C_{\mathcal{D}} = (\frac{sX}{s}, \frac{sY}{s})$
2: Decompose $\mathcal{D}$ into semi-shapes based on the interval $\Theta \in [0, 2\pi)$ and its centroid $C_{\mathcal{D}}$
3: Calculate the profile of semi-shapes $\zeta(\mathcal{D}, \Theta)$
4: $merit = [\,]$;
5: **for** $\theta = 1^\circ \ldots 359^\circ$ **do**
6: $\quad merit(\theta) = \Omega(\zeta(\mathcal{D}, 0^\circ), \zeta(\mathcal{D}, \theta))$;
7: **end for**
8: Detect $dPeaks \geq \tau$; *//the positive peaks of merit.*
9: **if** $length(dPeaks) > 0$ **then**
10: $\quad$ Determine $\psi = \overline{dPeaks}$;
11: $\quad \theta_0 = 360/length(dPeaks)$;
12: **else**
13: $\quad \psi = 0$; *//No symmetry found.*
14: **end if**

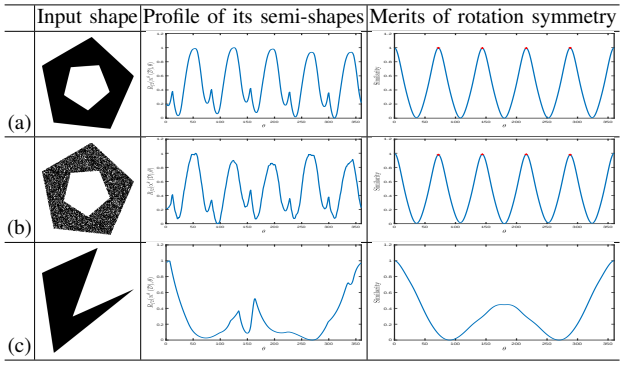

Fig. 7. Rotational symmetry measures ψ are 0.9913 and 0.9664 for shapes (a) and (b), while 0 is for shape (c).

periods. That means its rotational symmetry measure is 0 since the merit profile does not contain any positive peaks.

B. Evaluations of rotational symmetry detection

1) Detecting on single-contour shapes: MPEG-7 [26] is a conventional collection consisting of 1400 binary shapes of different objects for various analysis techniques, e.g., shape matching, shape description, etc. Initially, MPEG-7 is not aimed at tasks related to the rotational symmetry detection

GT	5 orders	5 orders	4 orders	3 orders
	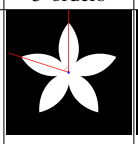	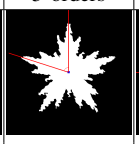	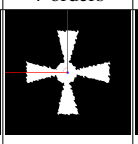	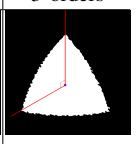
	(a)	(b)	(c)	(d)
Aguilar *et al.* [23]	#order ∈ $\{2, 4\}$	#order ∈ $\{2, 4\}$	#order ∈ $\{2, \mathbf{4}\}$	#order ∈ $\{2, 4\}$
Ours	$\theta_0 = \mathbf{72}^\circ$ #order = **5**	$\theta_0 = \mathbf{72}^\circ$ #order = **5**	$\theta_0 = \mathbf{90}^\circ$ #order = **4**	$\theta_0 = \mathbf{120}^\circ$ #order = **3**
GT	5 orders	8 orders	5 orders	4 orders
	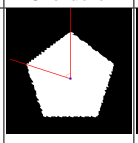	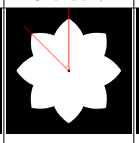	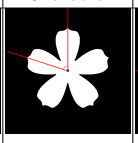	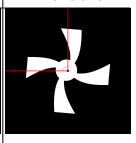
	(e)	(f)	(g)	(h)
Aguilar *et al.* [23]	#order ∈ $\{2, 4\}$	#order ∈ $\{2, 4, \mathbf{8}\}$	#order ∈ $\{2, 4\}$	#order ∈ $\{2, \mathbf{4}\}$
Ours	$\theta_0 = \mathbf{72}^\circ$ #order = **5**	$\theta_0 = \mathbf{45}^\circ$ #order = **8**	$\theta_0 = \mathbf{72}^\circ$ #order = **5**	$\theta_0 = \mathbf{90}^\circ$ #order = **4**

Fig. 8. Our results on MPEG-7's shapes compared to those of Aguilar *et al.* [23]. GT is a number of the ground-truth orders of shapes.

until Aguilar *et al.* [23] recently addressed it for their contour-based shape representation by using the Slope-Chain-Code (SCC) theory [24], [25] in order to represent the curve of binary shapes. This is because they realized that some MPEG-7's shapes have different orders of rotational symmetry, which are suitable for evaluating the performance of detectors.

Accordingly, we will evaluate the performance of our proposed detector on detecting the orders of these single-contour shapes in comparison with that of Aguilar *et al.* [23]. To this end, let us empirically consider the refining threshold $\tau = 0.85$ of our Algorithm 1 for detecting the orders of rotationally symmetrical shapes in MPEG-7 [26]. For the SCC-based representation, we follow the best parameters reported by Aguilar *et al.* [23], i.e., $M = 60$, $\epsilon = 0.15$, $\kappa = 0.82$, and $\rho = 0.1$, except $\Omega \in \{2, ..., M\}$. It should be noted that we set such Ω's values so that the SCC-based detector [23] can reach as many orders as possible. The function of the others could be referred to their work for more detail.

It can be observed in Fig. 8 that our proposed detector could efficiently detect all rotationally symmetrical shapes, as visualized in the red lines. Indeed, our algorithm correctly pointed out the orders and the rotation-symmetry angle of all shapes, including the deformation ones, i.e., shapes (b)-(e) in Fig. 8. In the meanwhile, the SCC-based one [23] just

Accepted by ICPR'2022

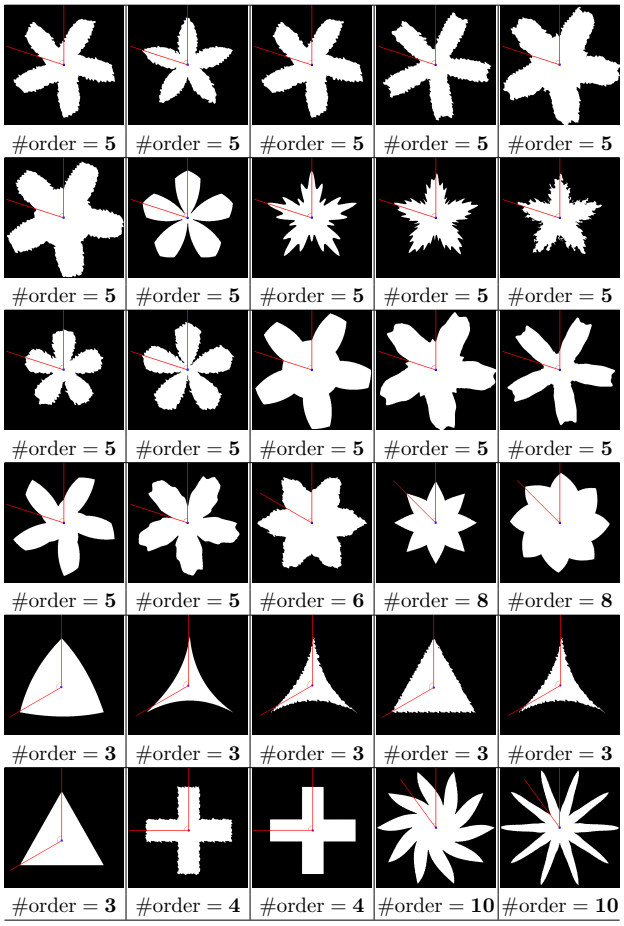

Fig. 9. Our results of orders on other MPEG-7's shapes.

GT	8 orders	4 orders	8 orders	5 orders
	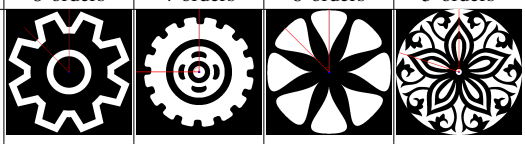			
	(a)	(b)	(c)	(d)
Aguilar *et al.* [23]	#order ∈ $\{2, 4, \mathbf{8}\}$	#order ∈ $\{2, \mathbf{4}, 8, 16\}$	**None** of #order	**None** of #order
Ours	$\theta_0 = \mathbf{45}^\circ$ #order = **8**	$\theta_0 = \mathbf{90}^\circ$ #order = **4**	$\theta_0 = \mathbf{45}^\circ$ #order = **8**	$\theta_0 = \mathbf{72}^\circ$ #order = **5**
GT	8 orders	6 orders	4 orders	4 orders
	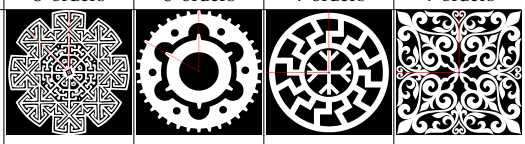			
	(e)	(f)	(g)	(h)
Aguilar *et al.* [23]	**None** of #order	**None** of #order	#order ∈ $\{2, \mathbf{4}\}$	#order ∈ $\{\mathbf{2}\}$
Ours	$\theta_0 = \mathbf{45}^\circ$ #order = **8**	$\theta_0 = \mathbf{60}^\circ$ #order = **6**	$\theta_0 = \mathbf{90}^\circ$ #order = **4**	$\theta_0 = \mathbf{90}^\circ$ #order = **4**

Fig. 10. Our results on compound shapes compared to those of Aguilar *et al.* [23]. GT is a number of the ground-truth orders of shapes.

Fig. 10(a) Fig. 10(b) Fig. 10(c) Fig. 10(d)

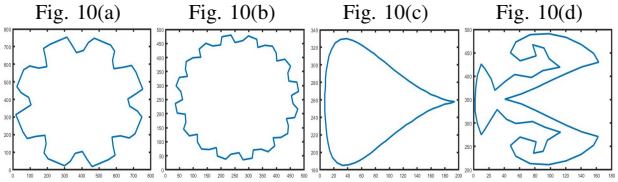

Fig. 11. Plots of SCC-based segments of the compound shapes (a), (b), (c), and (d) in Fig. 10, respectively.

listed their possible orders. It is noteworthy that in these output lists, the odd number of orders of the shapes was not in (see the results of shapes (a), (b), (d), (e), and (g) in Fig. 8). It means that the SCC-based detector has been in difficulty of the determination. In other words, it has failed in detecting the rotational symmetry properties on these shapes. More order results of our effective detection on other MPEG-7's shapes can be found in Fig. 9.

2) Detecting on compound-contour shapes: To the best of our knowledge, there is no dataset of compound-contour binary shapes for evaluating the rotational symmetry detectors. Therefore, we would like to collect 58 compound binary shapes from Internet (see Figs. 10 and 12). For this assessment, we also follow the same parameters, which were addressed for the aforementioned experiments on the single-contour shapes for the both detectors, i.e., ours and the SCC-based one [23].

It can be observed in Fig. 10 that our proposed detector also did well on all compound shapes (i.e., visualized in the red lines), while the SCC-based one [23] did not. Indeed, while ours pointed out the correct number of orders and the rotation angle of these shape, the SCC-based detector reported a list of possible orders. It should be noted that none of orders of shapes (c), (d), (e), and (f) in Fig. 10 was detected because of the limitation of the contour-based analysis, which will be discussed thoroughly in the below sub-section. More results of our effective detector on other compound shapes and those with a large number of orders can be found in Fig. 12.

3) Inadequacy of the contour-based analysis: Based on the experiments, we could assert the drawback of the contour-based detector [23] when facing with the compound shapes. Figs. 8 and 10 illustrate that the detector [23] only worked on the single-contour shapes, while ours did well on both. It is obvious that the contour-based detector has mostly failed on the compound shapes because of its inherent properties based on the SCC theory [24], [25] in the shape analysis. More concretely, the SCC-based algorithm has not well done due to the fact that it could not detect and represent all separate curves of the compound-contour shapes. It has practically formed one of the disjointed curves, i.e., a contour part of these shapes. Indeed, Fig. 11 illustrates that only one part of shapes (a), (b), (c), and (d) in Fig. 10 was segmented for the shape analysis. As a result, the SCC-based detector [23] had only addressed the outer contour of shapes (a) and (b) for its detection process. Here, there was an accidentally correct detection for shape (a) in Fig. 10 because of its inner circle-contour with notorious

Accepted by ICPR'2022

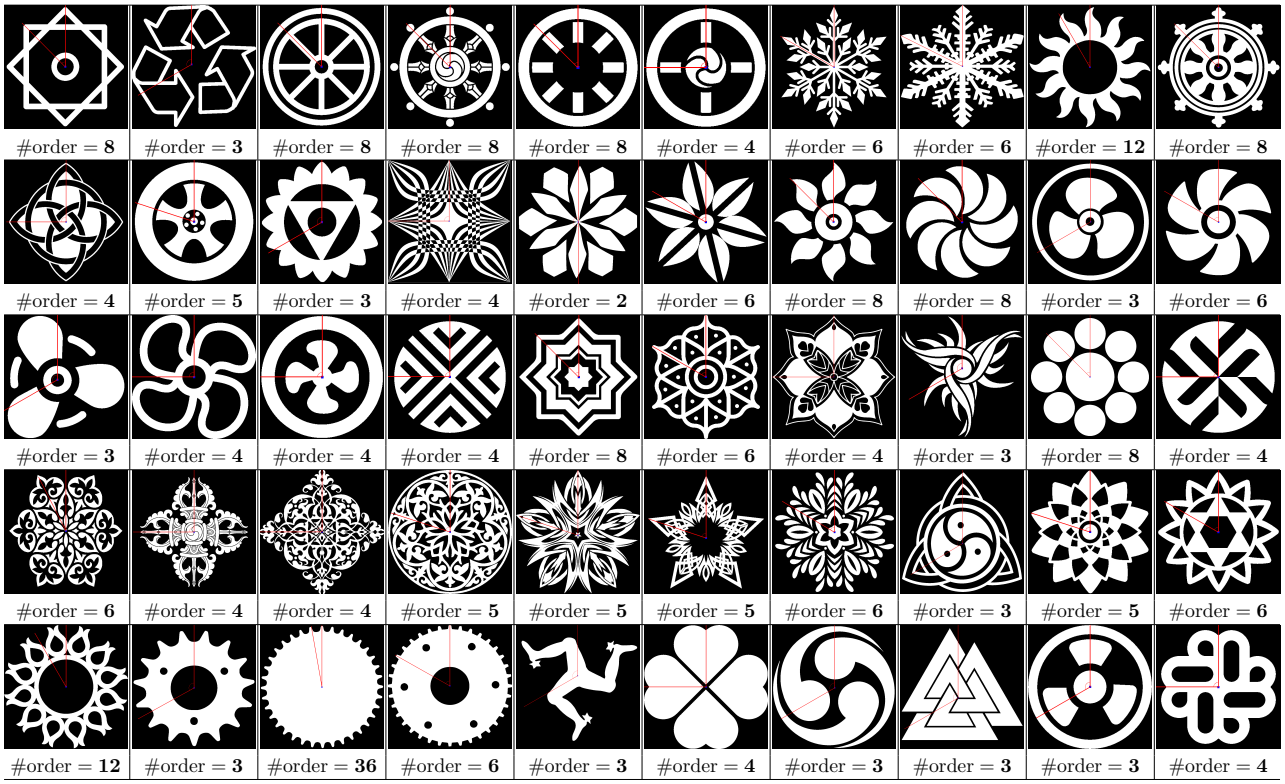

Fig. 12. Our detection results on other compound shapes and those with a large number of orders.

rotation-symmetry of myriad orders. In addition, the contour-based detector [23] has been arduous in handling the complex and decorative shapes (c) and (d) in Fig. 10 since just one part of its contour was located and segmented. Consequently, all the above analyses have validated the efficacy of our proposal.

C. Assessments of computational complexity

In regard to Algorithm 1, the proposed detector generally takes four main steps to detect the rotational symmetry of an arbitrary $\mathcal{N} \times \mathcal{N}$ shape $\mathcal{D}$. The complexity of determining the centroid of $\mathcal{D}$ is estimated as $\mathcal{Q}_{C_\mathcal{D}} \approx \mathcal{O}(\mathcal{N}^2)$. The complexity of the decomposition of $\mathcal{D}$ into semi-shapes $\zeta(\mathcal{D}, \Theta)$ is $\mathcal{Q}_{S_\mathcal{D}} = |\Theta| \times \mathcal{N} \times \mathcal{N}$, where $|\Theta|$ means the number of decomposing directions, i.e., $|\Theta| = 360$ in this case. Computing the profile of semi-shapes $\zeta(\mathcal{D}, \Theta)$, based on the Radon transform, takes $\mathcal{Q}_{\zeta_\mathcal{D}} = |\Theta| \times \mathcal{Q}_\mathcal{R}$, where $\mathcal{Q}_\mathcal{R} \approx \mathcal{O}(\mathcal{N}^2 \log \mathcal{N})$ denotes the complexity of the Radon transform (refer to [35] for estimations in detail). The detection and verification of rotational symmetry are done in $\mathcal{Q}_{\mathcal{V}_\mathcal{D}} \approx \mathcal{O}(|\Theta| + \mathcal{N})$. It should be noted that $|\Theta| = 360$ can be omitted because it is a constant value. Consequently, the complexity of our proposed detector is estimated as $\mathcal{Q}_{overall} \approx max(\mathcal{Q}_{C_\mathcal{D}}, \mathcal{Q}_{S_\mathcal{D}}, \mathcal{Q}_{\zeta_\mathcal{D}}, \mathcal{Q}_{\mathcal{V}_\mathcal{D}})$, i.e., $\mathcal{Q}_{overall} \approx \mathcal{O}(\mathcal{N}^2 \log \mathcal{N})$, compared to $\mathcal{O}(\Omega^2 M^2)$ of the SCC-based one [23]. In terms of computation time, it takes only 2.1s for our proposed detector to detect a rotationally symmetric 512×512 shape of MPEG-7 [26], while the SCC-based one needs up to 43.79s. All these time results are reported by the rough MATLAB codes on a Windows 10 64-bit laptop with core i7 2.6GHz and 16GB RAM.

V. Conclusions

We have proposed an effective method for rotational symmetry detection based on a novel concept of the semi-shape projection which allows constructing a profile of semi-shapes describing rotational symmetric properties of an arbitrary shape. Also, a new measure of rotational symmetry has been introduced to determine how good the rotational symmetry detection would be. Experiments on the single/compound binary shapes have validated the better performance in comparison with the recent work of Aguilar *et al.* [23]. In addition, based on the projection approach, our proposed algorithm can naturally deal with the compound shapes that are not evident for the existing contour-based method. This article is for the very first results on our research line. For perspectives, we will completely present the basic theories of the semi-shape projection as well as adequate assessments for rotational symmetry detection compared to the state of the art.

Acknowledgments

T.P. Nguyen is partially supported by CARTT, IUT de Toulon. This material is based upon work supported by the Air Force Office of Scientific Research under award number FA2386-20-1-4053.

REFERENCES

[1] H. Ogawa, "Symmetry analysis of line drawings using the Hough transform," *Pattern Recognition Letters*, vol. 12, no. 1, pp. 9–12, 1991.

[2] R. K. K. Yip, "A Hough transform technique for the detection of reflectional symmetry and skew-symmetry," *Pattern Recognition Letters*, vol. 21, no. 2, pp. 117–130, 2000.

[3] Y. Lei and K. C. Wong, "Detection and localisation of reflectional and rotational symmetry under weak perspective projection," *Pattern Recognition*, vol. 32, no. 2, pp. 167–180, 1999.

[4] L. Lucchese, "Frequency domain classification of cyclic and dihedral symmetries of finite 2-d patterns," *Pattern Recognition*, vol. 37, no. 12, pp. 2263–2280, 2004.

[5] V. S. N. Prasad and L. S. Davis, "Detecting rotational symmetries," in *ICCV*, 2005, pp. 954–961.

[6] G. Loy and J. Eklundh, "Detecting symmetry and symmetric constellations of features," in *ECCV*, vol. 3952, 2006, pp. 508–521.

[7] H. Cornelius and G. Loy, "Detecting rotational symmetry under affine projection," in *ICPR*, 2006, pp. 292–295.

[8] ——, "Detecting bilateral symmetry in perspective," in *CVPR*, 2006, p. 191.

[9] A. Martinet, C. Soler, N. Holzschuch, and F. X. Sillion, "Accurate detection of symmetries in 3d shapes," *ACM Trans. Graph.*, vol. 25, no. 2, pp. 439–464, 2006.

[10] H. Cornelius, M. Perdoch, J. Matas, and G. Loy, "Efficient symmetry detection using local affine frames," in *SCIA*, vol. 4522, 2007, pp. 152–161.

[11] S. Derrode and F. Ghorbel, "Shape analysis and symmetry detection in gray-level objects using the analytical Fourier-Mellin representation," *Signal Processing*, vol. 84, no. 1, pp. 25–39, 2004.

[12] M. M. Kazhdan, B. Chazelle, D. P. Dobkin, A. Finkelstein, and T. A. Funkhouser, "A reflective symmetry descriptor," in *ECCV*, 2002, pp. 642–656.

[13] N. Kiryati and Y. Gofman, "Detecting symmetry in grey level images: The global optimization approach," *International Journal of Computer Vision*, vol. 29, no. 1, pp. 29–45, 1998.

[14] M. Chertok and Y. Keller, "Spectral symmetry analysis," *IEEE Trans. Pattern Anal. Mach. Intell.*, vol. 32, no. 7, pp. 1227–1238, 2010.

[15] R. Nagar and S. Raman, "Reflection symmetry axes detection using multiple model fitting," *IEEE Signal Process. Lett.*, vol. 24, no. 10, pp. 1438–1442, 2017.

[16] ——, "Detecting approximate reflection symmetry in a point set using optimization on manifold," *IEEE Trans. Signal Process.*, vol. 67, no. 6, pp. 1582–1595, 2019.

[17] T. P. Nguyen, H. P. Truong, T. T. Nguyen, and Y.-G. Kim, "Reflection symmetry detection of shapes based on shape signatures," *Pattern Recognition*, vol. 128, p. 108667, 2022.

[18] J. Leou and W. Tsai, "Automatic rotational symmetry determination for shape analysis," *Pattern Recognition*, vol. 20, no. 6, pp. 571–582, 1987.

[19] J.-C. Lin, S.-L. Chou, and W.-H. Tsai, "Detection of rotationally symmetric shape orientations by fold-invariant shape-specific points," *Pattern Recognition*, vol. 25, no. 5, pp. 473–482, 1992.

[20] J. Flusser and T. Suk, "Rotation moment invariants for recognition of symmetric objects," *IEEE Transactions on Image Processing*, vol. 15, no. 12, pp. 3784–3790, 2006.

[21] R. K. K. Yip, "A Hough transform technique for the detection of parallel projected rotational symmetry," *Pattern Recognition Letters*, vol. 20, no. 10, pp. 991–1004, 1999.

[22] ——, "Genetic Fourier descriptor for the detection of rotational symmetry," *Image Vision Comput.*, vol. 25, no. 2, pp. 148–154, 2007.

[23] W. Aguilar, M. Alvarado-González, E. Garduño, C. Velarde, and E. Bribiesca, "Detection of rotational symmetry in curves represented by the slope chain code," *Pattern Recognit.*, vol. 107, p. 107421, 2020.

[24] E. Bribiesca, "A geometric structure for two-dimensional shapes and three-dimensional surfaces," *Pattern Recognit.*, vol. 25, no. 5, pp. 483–496, 1992.

[25] ——, "A measure of tortuosity based on chain coding," *Pattern Recognit.*, vol. 46, no. 3, pp. 716–724, 2013.

[26] L. J. Latecki, R. Lakämper, and U. Eckhardt, "Shape descriptors for non-rigid shapes with a single closed contour," in *CVPR*, 2000, pp. 1424–1429.

[27] T. P. Nguyen, "Projection based approach for reflection symmetry detection," in *ICIP*, 2019, pp. 4235–4239.

[28] S. Tabbone, L. Wendling, and J. Salmon, "A new shape descriptor defined on the Radon transform," *Computer Vision and Image Understanding*, vol. 102, no. 1, pp. 42–51, 2006.

[29] S. R. Deans, *The Radon Transform and Some of Its Applications*. Krieger Publishing Company, 1993.

[30] T. V. Hoang and S. Tabbone, "The generalization of the R-transform for invariant pattern representation," *Pattern Recognition*, vol. 45, no. 6, pp. 2145–2163, 2012.

[31] T. P. Nguyen and X. S. Nguyen, "Shape measurement using LIP-signature," *Computer Vision and Image Understanding*, vol. 171, pp. 83–94, 2018.

[32] T. P. Nguyen and T. V. Hoang, "Projection-based polygonality measurement," *IEEE Trans. Image Processing*, vol. 24, no. 1, pp. 305–315, 2015.

[33] T. P. Nguyen, X. S. Nguyen, M. A. Borgi, and M. K. Nguyen, "A projection-based method for shape measurement," *J. Math. Imaging Vis.*, vol. 62, no. 4, pp. 489–504, 2020.

[34] S. M. Stigler, "Francis Galton's Account of the Invention of Correlation," *Statistical Science*, vol. 4, no. 2, pp. 73–79, 1989.

[35] W. A. Götz and H. J. Druckmüller, "A fast digital radon transform–an efficient means for evaluating the hough transform," *Pattern Recognition*, vol. 29, no. 4, pp. 711–718, 1996.

Accepted by ICPR'2022